
The Dog Walking Theory: Rethinking Convergence in Federated Learning

Kun Zhai¹, Yifeng Gao¹, Xingjun Ma¹, Difan Zou², Guangnan Ye¹, Yu-Gang Jiang¹,

¹ Fudan University, Shanghai, China

² The University of Hong Kong, Hong Kong, China

{kdi22, yifenggao23}@m.fudan.edu.cn, {xingjunma, yegn, ygj}@fudan.edu.cn,
dzou@cs.hku.hk

Abstract

Federated learning (FL) is a collaborative learning paradigm that allows different clients to train one powerful global model without sharing their private data. Although FL has demonstrated promising results in various applications, it is known to suffer from convergence issues caused by the data distribution shift across different clients, especially on non-independent and identically distributed (non-IID) data. In this paper, we study the convergence of FL on non-IID data and propose a novel *Dog Walking Theory* to formulate and identify the missing element in existing research. The Dog Walking Theory describes the process of a dog walker leash walking multiple dogs from one side of the park to the other. The goal of the dog walker is to arrive at the right destination while giving the dogs enough exercise (i.e., space exploration). In FL, the server is analogous to the dog walker while the clients are analogous to the dogs. This analogy allows us to identify one crucial yet missing element in existing FL algorithms: the leash that guides the exploration of the clients. To address this gap, we propose a novel FL algorithm *FedWalk* that leverages an external easy-to-converge task at the server side as a *leash task* to guide the local training of the clients. We theoretically analyze the convergence of FedWalk with respect to data heterogeneity (between server and clients) and task discrepancy (between the leash and the original tasks). Experiments on multiple benchmark datasets demonstrate the superiority of FedWalk over state-of-the-art FL methods under both IID and non-IID settings.

1. Introduction

In recent years, federated Learning (FL) has emerged as a privacy-preserving training paradigm that allows multiple clients to collaboratively train a powerful global model without sharing their private data (Kairouz et al., 2021). It

has found impactful applications in biometrics (Aggarwal et al., 2021), healthcare (Sheller et al., 2020), and natural language processing (Ammad-Ud-Din et al., 2019), and has facilitated cross-device, cross-domain, and cross-institution collaborations. The fundamental idea of FL is to exchange gradients (or model parameters) rather than the raw training data to facilitate collaboration, which can effectively address the privacy concerns raised in traditional machine learning. However, exchanging gradients causes new problems such as high communication costs and slow convergence.

FedAvg (McMahan et al., 2017; 2016) is arguably one of the most widely adopted algorithms in FL. In FedAvg, a parameter server aggregates and averages the gradients of different clients obtained from their local training to update the global model. The updated global model can then be downloaded by the clients to initiate the next round of local training. As the model parameters are often of high dimensionality and large in size, frequently uploading and downloading the gradients (or model parameters) tends to incur expensive communication costs and latency. To tackle this issue, FedAvg typically increases the number of local updates on the client side and supports partial client participation in each communication round. However, this induces significant drifts of the clients from the global model, resulting in inaccurate gradient aggregation and slow convergence. Furthermore, theoretical analyses have revealed that the non-IID data distribution over different clients can also create gradient drift, which has become a major factor limiting the performance of FL in real-world applications (Li et al., 2019; Zhao et al., 2018).

A number of methods have been proposed to address the convergence issue of FL on non-IID data from roughly three different perspectives: 1) constraining the clients, 2) adaptive client selection, and 3) using pre-trained models. From the perspective of empirical risk minimization (ERM) (Malinovskiy et al., 2020; Wang et al., 2020b; Charles & Konečný, 2021; Zhang et al., 2022), several works have employed techniques like momentum (Das et al., 2022) and proximal terms (Li et al., 2020; Karimireddy et al., 2020; Acar et al., 2021) to constrain the direction of local client updates to be aligned with the global gradient. Client

selection is another important factor in FL convergence. Undoubtedly, random selection is not the optimal strategy as it tends to intensify the negative effect of data heterogeneity. By leveraging information such as client losses (Cho et al., 2020; Kim et al., 2020) and local updates (Ribero & Vikalo, 2020), an adaptive client selection strategy can effectively reduce the variance of the aggregated gradients. Meanwhile, the exploitation of pre-trained model parameters (on large-scale public datasets) is also a plausible choice for boosting the convergence of FL, as demonstrated in recent works (Nguyen et al., 2022; Chen et al., 2022).

Despite these works, the current literature still lacks a fundamental understanding of the key influencing factors on FL convergence.

In this paper, we propose the *Dog Walking Theory of Federated Learning* to analyze the convergence problem of FL. As shown in Figure 1, we view FL as a dog-walking process where the server acts as the dog walker while the clients act as the dogs. The goal is to make sure the dogs arrive at the right destination in the shortest time while getting enough exercise (i.e., good exploration of the space). The challenge here is how to ensure the dogs are under control and do not diverge from the main course. This is achieved by a proper leash in dog walking, yet has been ignored in current FL methods.

Based on the Dog Walking Theory, we provide a unified view of existing FL methods and identify most existing FL methods to be *passive FL* methods that do not have a server-side leash task to guide the convergence of the clients. Particularly, 1) FedAvg does not have any control over the clients (dogs), 2) optimization-based methods exploit historical trajectories to restrict the dogs, 3) client selection methods select a set of well-behaved dogs to lead the task, and 4) methods using pre-trained models hope to gain an advantage through a good starting point. Although these methods have demonstrated certain improvements over FedAvg, they do not have explicit leash guidance in their designs, missing one crucial element for FL convergence.

Motivated by the above analysis, we propose a novel FL algorithm **FedWalk** that adds an explicit “leash” into the existing FL paradigm. Specifically, FedWalk constructs a *leash task* at the server side based on a well-defined and easy-to-converge learning task on a public dataset. The leash task serves purely as a convergence guidance for the clients and thus can be different from the original task. This forms a dual-task learning framework between the server and the clients, with the client task being the original FL task while the leash (server) task is a centralized machine learning task. With the server-side leash task, FedWalk enjoys the advantages of both FL and centralized learning. More importantly, it fills the gap of missing “leash” in existing FL algorithms. We theoretically analyze the convergence of

FedWalk in comparison to FedAvg and empirically verify its superiority over existing FL methods. Our theoretical analysis helps to determine the extent to which the leash task should guide the client tasks.

In summary, we make the following main contributions:

- We introduce the *Dog Walking Theory* to help characterize the convergence of FL and identify one crucial yet missing element in current FL: a leash (task) that can guide the convergence of the clients. We also provide a unified view of existing FL algorithms as to how they address the “missing leash” problem.
- We propose a novel *FedWalk* algorithm that leverages an easy-to-converge leash task defined on a public dataset to guide the convergence of the clients. We theoretically analyze the convergence of *FedWalk* and derive a theoretical recommendation for the guiding strength (LLR) between the leash and client tasks.
- We empirically show that 1) *FedWalk* outperforms existing FL algorithms by a considerable margin under non-IID settings, 2) *FedWalk* can boost existing FL algorithms, and 3) *FedWalk* can also improve IID convergence.

2. Related work

Studies have shown that, although FedAvg can handle non-IID data to a certain extent (Li et al., 2019), degraded convergence is almost unavoidable when the clients’ data are non-IID (Zhao et al., 2018; Hsu et al., 2019). A body of work has been proposed to understand and mitigate the convergence issues of FL on non-IID data (Chen et al., 2020; Li et al., 2022b; Chen et al., 2023; Wu & Wang, 2022; Tan et al., 2023; Acar et al., 2021; Zhang et al., 2022; Li et al., 2021; Yuan et al., 2021; Crawshaw et al., 2024; Tan et al., 2022; Khanduri et al., 2021; Pathak & Wainwright, 2020). Here, we briefly review a subset of these methods that are most relevant to our work.

Optimization-based Methods. In distributed optimization, the widely used FL algorithm FedAvg is known as local SGD or parallel SGD (Zhou & Cong, 2017; Jain et al., 2018; Rosenblatt & Nadler, 2016; Zinkevich et al., 2010). From an optimization perspective, the convergence issue of FL is caused by the inconsistent local optima deviation from the global objective (Charles & Konečný, 2021; Wang et al., 2021; Malinovskiy et al., 2020). Therefore, the key to FL convergence is to align the optimization objectives between the client models and the global model. In traditional gradient descent optimization, the momentum technique can help accelerate convergence by accumulating a moving average of past gradients and using this accumulated information to update the model parameters. This has motivated the

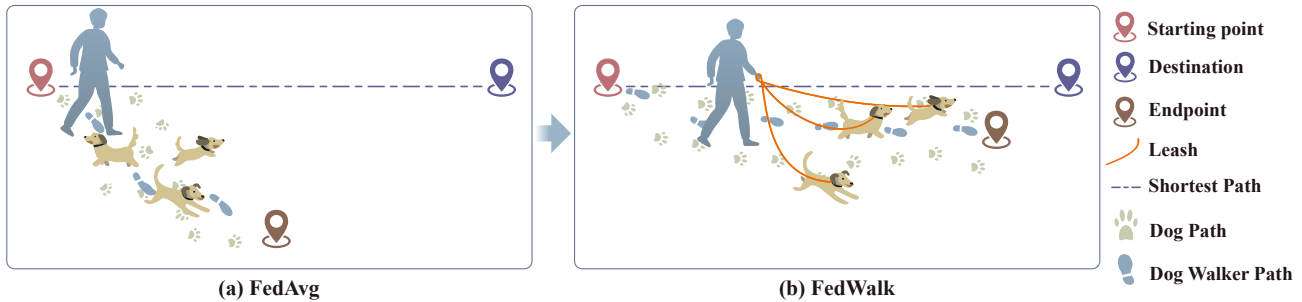


Figure 1. An illustration of the *Dog walking Theory* which formulates FL as a dog walking process where the dog walker is the server and the dogs are the clients. The goal is to arrive at the destination in the shortest possible time while giving the dogs enough exercise (space exploration). The leash plays a pivot role in achieving the goal.

adoption of momentum at the client side (Karimireddy et al., 2021; Xu et al., 2021), the server side (Wang et al., 2019; Reddi et al., 2020) or both (Khanduri et al., 2021; Das et al., 2022) to boost FL convergence on non-IID data. Momentum methods stabilize the FL process by leveraging historical information, i.e., it considers both the direction and magnitude of past updates to smooth out the fluctuations of the current update. This leads to an effective divergence reduction across the client models in FL. Moreover, the momentum technique can also be dynamic and adaptive, e.g., dynamically adjusting the momentum parameter during FL based on the observed gradients (Wu et al., 2023).

A few works proposed to exploit proximal terms to control the client updates, including FedProx (Li et al., 2020) and SCAFFOLD (Karimireddy et al., 2020). FedProx explicitly adjusts the direction of the client updates such that the local optimizations are performed in the vicinity of the global model (Li et al., 2020). This produces more stable local updates compared to FedAvg. Several variants of this method (Pathak & Wainwright, 2020; Nguyen et al., 2020) have been explored in follow-up works to achieve improved performance in autonomous driving (Donevski et al., 2021) and computer vision tasks (He et al., 2021). SCAFFOLD adjusts the update direction of the client according to the degree of client drift (Karimireddy et al., 2020). This restricts the most diverged local models from significantly influencing the global model, thus effectively boosting the convergence of FL on non-IID data.

Client Selection Methods. While random client selection is simple to deploy, it often undermines FL due to data and device heterogeneity (Li et al., 2022a). The most direct solution is to select "good" clients to participate in each round (Lai et al., 2021). Few works choose clients with higher local losses to accelerate the convergence of FL (Cho et al., 2020; Kim et al., 2020). Additionally, There are various methods for formulating clients' utility, such as client model weights (Ribero & Vikalo, 2020) and training time (Chai

et al., 2020). Oort (Lai et al., 2021), the state-of-the-art client selection method, presents a guiding client selection scheme that adopts utility-based strategies, considering both data and system heterogeneity. Client selection methods aim to utilize clients that exhibit superior convergence performance to enhance the overall convergence of federated learning (FL). However, consistently selecting prioritized clients leads to suboptimal performance because underrepresented clients may never have the opportunity to be selected. Hence, client selection methods should strike a balance between exploitation (prioritizing high-performing clients) and exploration (diversifying client selection) (Fu et al., 2023), mirroring principles found in optimization-based methods.

Pre-training-based Methods. In centralized machine learning, studies have shown that pre-trained weights on large-scale public datasets (Hendrycks et al., 2019; Devlin et al., 2018) can effectively boost the accuracy and robustness of the model. This is also the case for FL as demonstrated in recent research (Nguyen et al., 2022). In this case, FL with the pre-trained weights becomes a fine-tuning process that can effectively alleviate the divergence issue on non-IID data. FedPCL (Tan et al., 2022) further combines the pre-trained model with prototype learning and contrastive learning to construct a lightweight learning framework. The dependence of the pre-trained model on an external public dataset can also be reduced by using synthetic data, as verified in a recent study by Chen et al. (Chen et al., 2022). Non-IID data distribution across different clients increases the divergence of local models, leading to a widened gap between the aggregated model and the ideal model. Pre-trained models provide a better starting point for FL, reducing the distance between the initial and optimal model compared to random initialization.

The above methods address the convergence issues of FL on non-IID data by either restricting (or ignoring) the local updates that diverge drastically from the global average or leveraging pre-trained weights to stabilize the convergence

process. In this work, we identify one crucial yet missing element in existing FL methods that motivates a novel FL method toward improved performance on non-IID data.

3. Proposed Method

We first introduce the *Dog Walking Theory*, based on which we provide a unified view of existing FL methods. We then describe the proposed FedWalk algorithm.

3.1. The Dog Walking Theory of FL

As illustrated in Figure 1, we introduce a *Dog Walking Theory* to format FL as a process of dog walking where the goal of the dog walker is to move from one side of the park to the other while giving the dogs enough exercise. In FL, the server can be viewed as the dog walker while the clients can be viewed as the dogs. By analogy, the goal of FL is to converge to the global optimal while allowing the clients to freely update their local models based on their private data. An informal definition of the *Dog Walking Theory of Federated Learning* is as follows:

Theorem 3.1. (*Dog Walking Theory of Federated Learning*) *Federated learning with a parameter server and multiple clients is a dog-walking process with the server being the dog walker, the clients being the dogs, and the goal is to leash walk the dogs to a destination while having a flexible exploration of the space.*

Following the above theory, we can discuss the sub-goals of each component of FL. The dog walker does not want to lose control of the dogs as otherwise he/she will fail to arrive at the destination, while the dogs do not want any constraint from the dog walker and want to explore the space freely. The leash plays a central role in balancing the two sub-goals. By adjusting the leash, the dog walker can have proper control over the dogs while giving sufficient flexibility to the dogs. It is worth mentioning that, the concept of *Dog Walking Theory* has been discussed in economics and capital market¹ to describe the relationship between prices and values, i.e., prices ultimately regress to values. In our work, the *Dog Walking Theory of Federated Learning* formulates a form of multi-party constrained cooperation.

3.2. A Unified View of Existing FL Methods

Based on the *Dog Walking Theory*, we provide a unified view of existing FL methods designed to address the convergence issue of FL. In the most classic FL algorithm FedAvg, each client (dog) has its own private data and local objective, thus can freely explore its local space as much as determined by the local epochs — a hyper-parameter defining the number of local update epochs within each communication round.

¹<https://stockstotrade.com/trading-first-steps/>

As FedAvg takes the averaged local models as the global model, the dog walker (server) in FedAvg does not have any control over the dogs (clients) as illustrated in Figure 1(a). Moreover, the dogs under the non-IID setting are more diverged and random than those under the IID setting. In this case, FedAvg can be easily distracted by outlier clients and fails to converge to the global optimum.

As reviewed in Section 2, existing convergence acceleration methods for FL include optimization-based methods, client selection methods, and methods that use pre-trained models. Optimization-based methods such as FedProx (Li et al., 2020), SCAFFOLD (Karimireddy et al., 2020), FedDyn (Acar et al., 2021), and FedGLOMO (Das et al., 2022) exploit historical gradients to constrain the direction of the client updates. This constraint can be interpreted as restricting the dogs to be close to each other so as to avoid digression, which limits the freedom of the clients and the effectiveness of local training. Client selection methods, on the other hand, mitigate the adverse effects of data heterogeneity by adaptively selecting clients that benefit the convergence the most. This strategy is to force other dogs to follow a set of well-behaved dogs. The guidance provided by both types of methods originates from the dogs (clients) themselves, thus can together be viewed as one type of *self-guidance*. However, methods that use pre-trained models are different, as the pre-trained weights (on a public dataset) represent the utilization of external information to initialize (but not guide) the local training. This can be interpreted as setting up a good starting point. As such, these methods can only help the early stage of the training process.

We call an FL method *passive FL* method if its global model is aggregated from the local models rather than directly specified by the server. The above FL methods all fall into this category. With this view, we identify a crucial yet missing element in passive FL methods: the leash that provides active control over the clients. We call FL methods that have a server-side *leash task* guiding the convergence of the clients *active FL* methods. We argue that the leash task is an essential part of FL and can be easily defined based on a public dataset. We expect *active FL* methods to replace passive FL methods in most FL applications. Moreover, any passive FL method can be converted into an active FL method by directly plugging in a leash task. Next, we will introduce the proposed active FL method *FedWalk*.

3.3. FedWalk

Problem Definition. Consider a standard FL setting following (McMahan et al., 2017; 2016), which contains N clients and a central server. Client $k \in [N]$ has its local dataset D_k . Note that D_k may differ across different clients, which corresponds to client heterogeneity. Let f_k be the local objective of the k -th client: $f_k = \mathbb{E}_{\xi_k \sim D_k} [\mathcal{L}(\mathbf{W}; \xi_k)]$.

FL is to learn a machine learning model \mathbf{W} over dataset $D = \cup_{k \in [N]} D_k$, by solving the following empirical risk minimization (ERM) problem:

$$\min_{\mathbf{W}} \left\{ f(\mathbf{W}) = \sum_{k=1}^N p_k f_k(\mathbf{W}) \right\}, \quad (1)$$

where p_k is the importance of the k -th client and $\sum_{k=1}^N p_k = 1$. The notations used in this paper are summarized in Table 1.

Algorithm Description. *FedWalk* has two main steps: (1) the server collaborates with clients to optimize the FL task, and (2) the server optimizes the leash task. And the leash task guides the optimization of the FL task. We describe each step in detail below.

During the learning process, the server needs to possess three types of information: 1) the global model \mathbf{W}_t , 2) the training data of the leash task selected from a public dataset, and 3) the training loss of the client models \mathcal{L}^c . During the t -th communication round, the server broadcasts the global model \mathbf{W}_t to the selected clients $C \subseteq [N]$. Then, the clients start to **optimize the FL task** locally as follows. The client $k \in C$ first initializes its local model with the received global model $\mathbf{V}_k = \mathbf{W}_t$. It then performs local updates as:

$$\mathbf{V}_k = \mathbf{V}_k - \eta_t \nabla f_k(\mathbf{V}_k, \xi_k) \quad (2)$$

$$\mathcal{L}_k = \mathcal{L}(\mathbf{V}_k, D_k), \quad (3)$$

where ξ_k is a sample uniformly chosen from the local dataset D_k , \mathcal{L}_k is the training loss of k -th client on training data D_k .

After a certain number of local updates, the clients upload their accumulated updates to the server which then aggregates the local updates and calculates the momentum local losses:

$$\bar{\mathbf{W}}_t = \frac{1}{m} \sum_{k \in C} \mathbf{V}_k \quad (4)$$

$$\mathcal{L}^c = \beta * \mathcal{L}^c + (1 - \beta) \frac{1}{m} \sum_{k \in C} \mathcal{L}_k. \quad (5)$$

The next step is to **optimize the leash task**. Specifically, the server updates the global model (obtained after the above aggregation) following:

$$\bar{\mathbf{W}}_t = \bar{\mathbf{W}}_t - \gamma_t \nabla F(\bar{\mathbf{W}}_t, \xi). \quad (6)$$

As the leash task only serves the purpose of convergence guidance and could be different from the FL task, it is thus important to make sure the two tasks do not conflict with each other. To this end, we propose the following *Log Loss Ratio* (LLR) constraint to balance the two tasks:

$$\log\left(\frac{\mathcal{L}^c}{\mathcal{L}^s}\right) < \tau, \quad (7)$$

where \mathcal{L}^s is the loss of the leash task and τ is a hyper-parameter that upper bounds the LLR. After the leash optimization, the server obtains an updated new global model for the t -th communication round: $\mathbf{W}_{t+1} = \bar{\mathbf{W}}_t$. The detailed optimization steps are summarized in Algorithm 1.

Importance of the LLR Constraint. The log loss ratio $\log\left(\frac{\mathcal{L}^c}{\mathcal{L}^s}\right)$ in Eq. (7) acts as an indicator of the guiding strength. A higher LLR leads to a low loss (\mathcal{L}^s) of the leash task, i.e., more guiding strength from the leash task. Although the leash task can be carefully chosen such that it is well-defined (by a public dataset) and easy-to-converge, it only serves the purpose of convergence acceleration by producing a more flat loss landscape and can be completely irrelevant to the FL task. In this case, an overly large guiding strength (higher LLR) could lead to a biased global model towards the leash task. It is thus crucial to carefully choose the τ hyper-parameter to achieve both accelerated convergence and improved generalization. In Section 4, we will make recommendations according to our theoretical analysis.

Leash Task Selection Selecting the right leash task is the key to the success of FedWalk. Arguably, the lower the heterogeneity between the leash and the FL tasks, the better the guiding effect. In an extreme case where the two tasks are identical, FL becomes the traditional machine learning where the server possesses the full training dataset. In a general case, the two tasks are different. In this case, the leash task can be selected to be a similar type of learning task as the FL task but having a public training dataset available. Intuitively, the more similar the leash task to the FL task, the better the convergence. The selection process only needs to analyze the task information (e.g., class names) of the FL task, thus, it can be easily automated with the help of a large language model (LLM). Taking FL on the CIFAR-10 dataset as an example, we could select a few (e.g., 20) classes from the ImageNet-1K dataset to form the leash task. In our experiment, we test three different selection strategies based on GPT-4 according to the degree of concept overlap between the leash and FL tasks, as detailed in Section 5.1. It is possible that in practice, some FL tasks can find leash tasks with low heterogeneity, while others cannot. We believe this challenge can be largely addressed by powerful generative models like stable diffusion (Rombach et al., 2022) and GPT-4 (Achiam et al., 2023).

4. Convergence Analysis

Here, we analyze the convergence of FedWalk and the key influencing factors. We first describe assumptions and definitions used in the convergence analysis, and then we give the convergence result and remarks. The details of the proof are given in the Appendix.

Algorithm 1 FedWalk

Input: initial global model weight \mathbf{W}_0 ; k -th client local model weight \mathbf{V}_k ; client loss value \mathcal{L}^c ; leash task loss value \mathcal{L}^s ; client learning rate η_t ; leash task learning rate γ_t ; total client number N ; total round number T ; client step number T_c ; leash task step number T_s ; client data $\{D_1, D_2, \dots, D_N\}$; leash task data D_s ; threshold τ ; momentum β

Output: global model weight \mathbf{W}_T

```

1  $\mathcal{L}^c = 0$ ;
   for each round  $t = 1, 2, \dots, T$  do
2   sample  $m$  clients  $C \subseteq \{1, 2, \dots, N\}$ 
3   broadcasts  $\mathbf{W}_{t-1}$  to all clients  $k \in C$ 
4   # clients and server optimizes FL task :
5   for all client  $k \in C$  in parallel local_update do
6      $\mathcal{L}_k, \mathbf{V}_k = \text{local\_update}(\mathbf{W}_{t-1}, \eta_t, D_k)$ 
7   end
8   server aggregates:
      $\bar{\mathbf{W}}_t = \frac{1}{m} \sum_{k \in C} \mathbf{V}_k$ 
      $\mathcal{L}^c = \beta * \mathcal{L}^c + (1 - \beta) \frac{1}{m} \sum_{k \in C} \mathcal{L}_k$ 
9   # server optimizes leash task :
10  if  $\log(\frac{\mathcal{L}^c}{\mathcal{L}^s}) < \tau$  then
11    for each server step  $t_s = 1, 2, \dots, T_s$  do
12      compute min-batch gradient  $\mathbf{q}(\bar{\mathbf{W}}_t)$ 
13       $\bar{\mathbf{W}}_t = \bar{\mathbf{W}}_t - \gamma_t \mathbf{q}(\bar{\mathbf{W}}_t)$ 
14    end
15     $\mathcal{L}^s = \mathcal{L}(\bar{\mathbf{W}}_t, D_s)$ 
16  end
17  $\mathbf{W}_t = \bar{\mathbf{W}}_t$ 
    
```

4.1. Assumption and Definition

We make the following assumptions on the functions f_1, \dots, f_N , with typical examples being ℓ_2 -norm regularized linear regression, logistic regression, and softmax classifier.

Assumption 4.1. f_1, \dots, f_N and F are all L -Smooth: for all V and W , $f_k(V) \leq f_k(W) + (V - W)^\top \nabla f_k(W) + \frac{L}{2} \|V - W\|_2^2$.

Assumption 4.2. f_1, \dots, f_N and F are all μ -Strong convex: for all V and W , $f_k(V) \geq f_k(W) + (V - W)^\top \nabla f_k(W) + \frac{\mu}{2} \|V - W\|_2^2$.

Assumption 4.3. Let ξ_t^k be sampled from k -th client's local data uniformly at random. The variance of stochastic gradients in each client is bounded: $\mathbb{E}[\|\nabla f_k(\mathbf{V}_t^k, \xi_t^k) - \nabla f_k(\mathbf{V}_t^k)\|^2] \leq \sigma_k^2$ for $k=1, 2, \dots, N$.

Assumption 4.4. Let ξ_t^s be sampled from server data uniformly at random. The variance of stochastic gradients is bounded:

$$\mathbb{E}[\|\nabla F(\bar{\mathbf{W}}_t, \xi_t^s) - \nabla F(\bar{\mathbf{W}}_t)\|^2] \leq \sigma_s^2.$$

Def local_update(\mathbf{W}, η, D):

```

initialize local model  $\mathbf{V} = \mathbf{W}$ 
for each client step  $t_c = 1, 2, \dots, T_c$  do
  compute mini-batch gradient  $\mathbf{g}(\mathbf{V})$ 
   $\mathbf{V} = \mathbf{V} - \eta \mathbf{g}(\mathbf{V})$ 
end
 $\mathcal{L}_{local} = \mathcal{L}(\mathbf{V}, D)$ 
Return  $\mathcal{L}_{local}, \mathbf{V}$ 
    
```

Table 1. Summary of the notation used in the paper

N, m and k	total number, sample number, and client index
(T, t)	number, index of communication rounds,
(T_c, t_c)	number, index of client local steps
(T_s, t_s)	number, index of leash task steps
$\bar{\mathbf{W}}_t$	aggregated model in round t
\mathbf{W}_t	global model in round t
\mathbf{V}_t^k	k -th client's local model in round t
$\mathcal{L}(\mathbf{W}, D)$	loss function on model \mathbf{W} and data D
\mathcal{L}^c and \mathcal{L}^s	loss value of the FL and leash task
\mathbf{g}_t^k and \mathbf{q}_t	min-batch gradient of k -th client, leash task in round t
f, f_k and F	function of global, k -th client and leash
$\mathbf{W}^*, \mathbf{W}_s^*$ and \mathbf{V}_k^*	the optimal solution of global model, leash model and k -th client model
η_t and γ_t	learning rate of client local and leash task in round t
p_k	importance of the k -th client
τ	the threshold for $\frac{\mathcal{L}^c}{\mathcal{L}^s}$

Assumption 4.5. The expected squared norm of stochastic gradients is uniformly bounded, i.e., $\mathbb{E}[\|\nabla f_k(\mathbf{V}_t^k, \xi_t^k)\|^2] \leq G^2$ for all $k=1, 2, \dots, N$ and $t=1, 2, \dots, T-1$.

Definition 4.6. [FL data heterogeneity] Let f^* and f_k^* be the optimum of f and f_k , respectively. We use $\Gamma = f^* - \sum_{k=1}^N p_k f_k^*$ to quantify the degree of data heterogeneity in the FL task. If the data is IID, then Γ goes to zero as the number of samples grows. If the data is non-IID, then Γ is nonzero, and its magnitude measures the heterogeneity of the data distribution.

Definition 4.7. [Leash-FL data heterogeneity.] Let F^* be the optimum of the leash task F , the data heterogeneity between the leash and FL tasks are defined as $\Gamma_s = f^* - F^*$. If the data is IID between the FL and the leash tasks, then $\Gamma_s = 0$. If the data is non-IID, then Γ_s is nonzero and its magnitude measures the heterogeneity between the two tasks.

Definition 4.8. [Leash-FL task discrepancy.] Let $\bar{\mathbf{W}}_t$ be the aggregated model in the t -th communication round, the discrepancy between the leash and FL tasks is defined as $\Pi = F(\bar{\mathbf{W}}_t) - f^*$, where $F(\bar{\mathbf{W}}_t)$ is the performance of the

aggregated model on the leash task and f^* is the optimal global function of the FL task.

4.2. Convergence Result

Here, we analyze the case of full participation where all the clients participate the global aggregation. Following (Li et al., 2019), we let $\Delta_{t+1}^{FedWalk} = \mathbb{E}[\|\mathbf{W}_{t+1} - \mathbf{W}^*\|^2]$. Note that $\mathbf{W}_{t+1} = \mathbf{W}_t - \eta_t \mathbf{g}_t - \gamma_t \mathbf{q}_t$ and $\Delta_{t+1}^{FedAvg} = \mathbb{E}[\|\mathbf{W}_t - \mathbf{W}^* - \eta_t \mathbf{g}_t\|^2]$.

Theorem 4.9. *Let Assumptions 4.1 to Assumptions 4.5 hold and $\eta_t \leq \frac{1}{4L}$, we have*

$$\Delta_{t+1}^{FedWalk} = \Delta_{t+1}^{FedAvg} + \epsilon$$

where

$$\epsilon = \gamma_t^2 \sigma_s^2 + \left(\frac{2}{\mu} + 4L\gamma_t^2 - 4\gamma_t\right)\Gamma_s - 4\gamma_t(1 - L\gamma_t)\Pi$$

with $\Gamma_s = f^* - F^*$, $\Pi = F(\bar{\mathbf{W}}_t) - f^*$, and $\gamma_t < \frac{1}{L}$

Remark 4.10. Theorem 4.9 reveals that FedWalk has an extra term ϵ in its update steps compared to FedAvg. If $\epsilon \leq 0$, FedWalk converges faster than FedAvg; however, if $\epsilon > 0$, it converges slower. Thus, to obtain faster convergence, we need to guarantee $\epsilon \leq 0$, that is:

$$\Pi \geq \frac{\gamma_t^2 \sigma_s^2 + \left(\frac{2}{\mu} + 4L\gamma_t^2 - 4\gamma_t\right)\Gamma_s}{4\gamma_t - 4L\gamma_t^2}. \quad (8)$$

This means the Leash-FL task discrepancy Π cannot be too small as otherwise, the FL model will converge to the leash task.

Guiding Strength. Throughout the training process of FedWalk, the leash task extends guidance to the FL task to help convergence. Mathematically, this relationship is represented by the formula $\Pi = F(\bar{\mathbf{W}}_t) - f^*$, where Π denotes Leash-FL task discrepancy. Here, f^* represents the optimal solution of the FL task, while F is the leash function acting on the aggregated model parameters ($\bar{\mathbf{W}}_t$). A decrease in Π indicates a closer alignment of ($\bar{\mathbf{W}}_t$) with the optimal model of the leash task.

A smaller Π reflects an intensified guiding strength exerted by the leash task on the model ($\bar{\mathbf{W}}_t$). However, an excessive guiding strength may pull ($\bar{\mathbf{W}}_t$) to be overly close to the leash task, thereby drifting away from the original FL task. This misalignment conflicts with the initial purpose of the leash task, i.e., helping the FL task. It is thus crucial to constrain the guiding strength within a proper range.

Eq. (8) delineates an upper bound on the guiding strength. Key determinants impacting the value of Π encompass γ_t , σ_s , L , μ and Γ_s . Among these, L , μ , and σ_s are constants. With a consistent learning rate γ_t , the Leash-FL data heterogeneity Γ_s emerges as the predominant influencing factor

on Π . As Γ_s escalates, so does the lower bound of Π , indicating a proportional decrease in the guiding strength of the leash task. Conversely, as Γ_s diminishes, the lower bound of Π decreases, indicating an increase in the guiding strength of the leash task.

Remark 4.11. If the leash task does not provide guidance to the FL task, it follows $\epsilon = 0$, where $\gamma_t = 0$ and $\Gamma_s = 0$. In this case, we have:

$$\Delta_{t+1}^{FedWalk} = \Delta_{t+1}^{FedAvg}.$$

Remark 4.11 guarantees the independence of the leash task in the algorithm. Therefore, FedWalk is not only able to improve efficiency with the leash task but still maintains the same theoretical guarantees as FedAvg without the leash task.

Remark 4.12. The Leash-FL data heterogeneity Γ_s has a significant effect on the convergence of FedWalk, with better convergence observed when the heterogeneity decreases. In the ideal case of zero heterogeneity ($\Gamma_s = 0$), we have:

$$\Delta_{t+1}^{FedWalk} = \Delta_{t+1}^{FedAvg} + \epsilon$$

where

$$\epsilon = \gamma_t^2 \sigma_s^2 - 4\gamma_t(1 - L\gamma_t)\Pi \leq 0.$$

As σ_s approaches 0 and $\eta_t \leq \frac{1}{4L}$, ϵ turns negative. This indicates that the guidance offered by the leash task is consistently advantageous. This result can be intuitively interpreted as the leash task is defined on all clients' data. In this case, the centralized training updates from the leash task offer a superior and much more efficient update direction compared to the heterogeneous nature of the clients.

5. Experiments

In this section, we first describe the experimental setup and then compare FedWalk with SOTA FL methods. We also conduct an ablation analysis of our FedWalk.

5.1. Experimental Setup

Datasets and Models. We consider two commonly used benchmark datasets for FL, i.e., CIFAR-10 and CIFAR-100 datasets (Krizhevsky et al., 2009) with heterogeneous dataset partition. Following prior work (Li et al., 2022b), we use Dirichlet distribution $\text{Dir}(\alpha)$ to simulate the non-IID setting, with smaller α indicating higher data heterogeneity. In our main experiment, we set $\alpha = 0.1$ (non-IID) and $\alpha = 10$ (IID) for CIFAR-10, $\alpha = 0.01$ (non-IID) and $\alpha = 100$ (IID) for CIFAR-100. For both CIFAR-10 and CIFAR-100, we employ ResNet18 (He et al., 2016) pre-trained on ImageNet-1k as the basic model. See the appendix for more details.

Table 2. The average training and test accuracies (%) of different methods, including the baselines, FedWalk, and their combinations, on CIFAR-10 and CIFAR-100 datasets under both non-IID and IID settings. Blue/red color indicates an increase/decrease.

Method	CIFAR-10				CIFAR-100			
	non-IID (Dir(0.1))		IID		non-IID (Dir(0.01))		IID	
	Training	Test	Training	Test	Training	Test	Training	Test
Fedavg	92.66	88.06	99.99	95.58	67.13	58.53	99.97	80.03
SCAFFOLD	84.92	82.84	100	94.99	62.17	52.66	99.12	78.59
FedProx	90.97	85.23	99.99	95.48	67.18	58.72	99.98	80.13
FedNova	91.70	86.32	99.99	95.46	69.93	60.12	99.98	80.11
FedWalk	95.26(+2.6)	91.45(+3.39)	100(+0.01)	95.88(+0.03)	71.22(+4.09)	61.35(+2.83)	99.98(+0.01)	80.38(+0.35)
SCAFFOLD + FedWalk	94.05(+9.13)	86.48(+3.64)	99.99(-0.01)	96.58(+1.59)	69.17(+7)	57.04(+4.38)	99.93(+0.81)	82.46(+3.87)
FedProx + FedWalk	95.55(+4.58)	91.41(+6.18)	99.99(+0)	95.82(+0.34)	71.11(+3.93)	61.65(+2.92)	99.98(+0)	80.84(+0.71)
FedNova + FedWalk	96.63(+4.93)	91.89(+5.57)	100(+0.01)	95.82(+0.36)	73.88(+3.95)	63.27(+3.15)	99.98(+0)	80.84(+0.73)

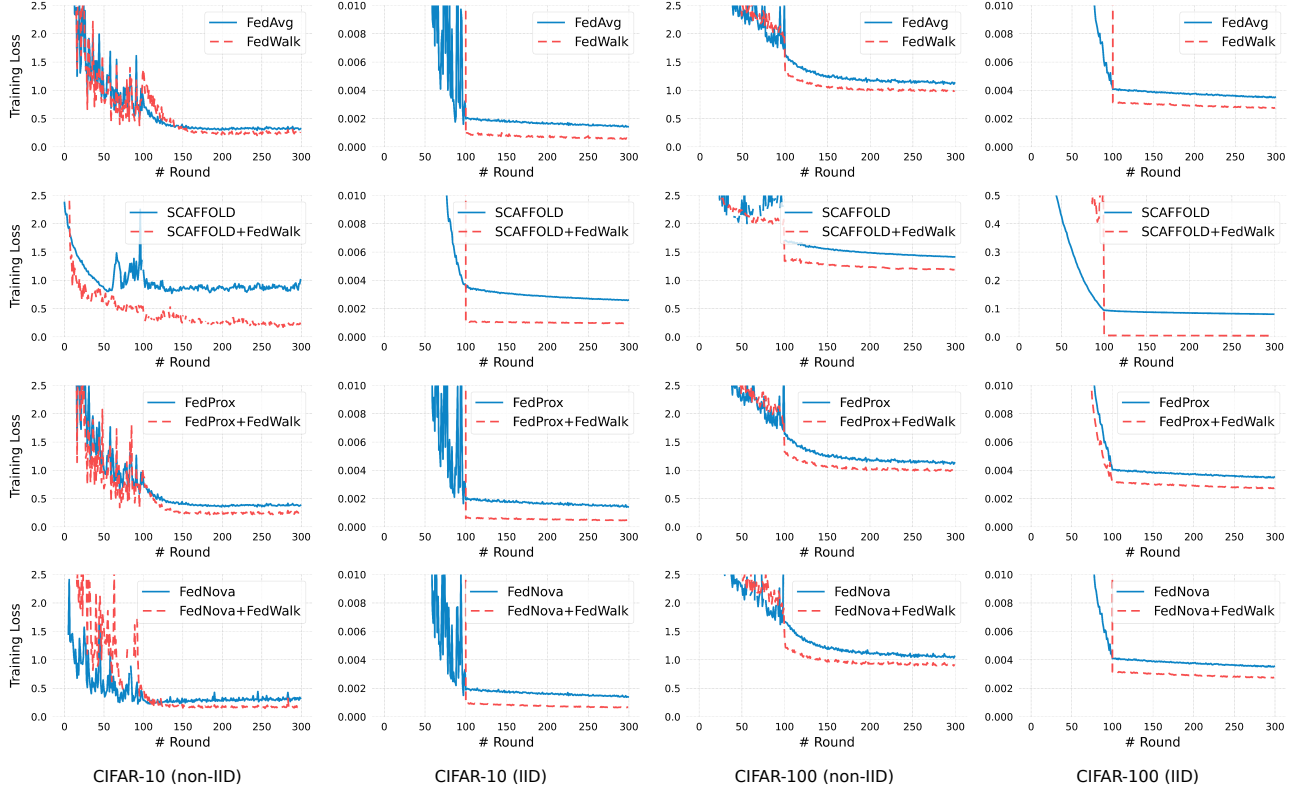


Figure 2. The training losses of different methods across 300 communication rounds on CIFAR-10 and CIFAR-100 datasets under IID and non-IID settings.

Baselines. We consider 4 FL baselines: 1) *FedAvg* (McMahan et al., 2017) which is a classic FL algorithm; 2) *SCAFFOLD* (Karimireddy et al., 2020) which introduces variance among the clients and corrects the local updates by adding the drift into the local training; 3) *FedProx* (Li et al., 2020) which improves local objective optimization by constraining the divergence between the local and the global models; and 4) *FedNova* (Wang et al., 2020a) which normalizes and scales the local updates to eliminate object inconsistency while maintaining convergence.

FedWalk. We use ImageNet-1K to define the leash task,

which applies to a range of vision applications. Specifically, we explore three types of leash tasks: 1) HH (high heterogeneity), MH (medium heterogeneity), and LH (low heterogeneity). Specifically, for CIFAR-10, we construct the LH leash task by asking GPT-4 to find the top 20 ImageNet classes that share the most similar concepts with the FL task. For the MH leash task, we replace the top 10-20 classes with 10 randomly selected ImageNet classes, while for the HH leash task, we randomly select 20 classes from ImageNet. For CIFAR-100, we only construct an LH leash task of 40 classes following the same procedure. Note that the entire

construction process only needs the class names. For all leash tasks, we adopt local steps $T_s = 1$, batch size 64, and learning rate $\gamma_t = \eta_t$. We set $\tau = [0, 0.5, 1]$ for CIFAR-10 LH and CIFAR-100 leash tasks, $\tau = [-1, -0.5, 0]$ for CIFAR-10 MH leash task, $\tau = [-1.3, -1.1]$ for CIFAR-10 HH leash task.

Hyper-parameters. For all FL methods, we set the total client number to $N = 100$, the sampled client number to $m = 20$, and the total communication round to $T = 300$. For the FL tasks, local steps are set to $T_c = 5$ with batch size 32, the learning rate is set to $\eta_t = [1e-2, 1e-3, 1e-4]$ when $t < 100$, $\eta_t = 1e-5$ otherwise. The base of $\log(\cdot)$ in LLR is 2. In each experiment, the global model with the highest accuracy is selected as the final model.

5.2. Main Results

Here, we report the results with the LH leash task while deferring the results of other leash selections to Section 5.3. As shown in Table 2, FedWalk achieves a considerable performance improvement over the baselines, surpassing the best baseline by at least 3.39 % and 1.24% test accuracy on CIFAR-10 and CIFAR-100 dataset under the non-IID Dir(0.1) setting. When combined with the baselines, FedWalk can boost their test accuracy consistently across different scenarios. Particularly, on CIFAR-10 dataset under the non-IID setting, it improves the test accuracy of SCAFFOLD, FedProx, and FedNova by 3.64%, 6.18%, and 5.57%, respectively. A similar trend is also observed on CIFAR-100 and the IID settings. An exception occurs with the training accuracy of SCAFFOLD + FedWalk on CIFAR-10 under the IID setting, where there is a 0.01% decrease. We conjecture that this is caused by the randomness of the optimization.

We further show the training losses of different methods in Figure 2, where FedWalk exhibits an evident convergence acceleration compared to the baselines under both IID and non-IID settings. One interesting observation is that under the non-IID setting, the leash task appears to hinder the convergence of the FL task during an early guiding process (i.e., before 100 communication rounds). This suggests an inherent tension between the leash and FL tasks. Such a tension turns out to benefit the convergence at a later stage as indicated by the lower training loss. This reveals the working mechanism of FedWalk to some extent.

5.3. Ablation Study

Here, we conduct three sets of ablation experiments on CIFAR-10 to provide more understanding of FedWalk.

(1) Impact of τ . The guiding strength in FedWalk is controlled by the hyper-parameter τ . In Figure 3, we show the correlation between τ and the model’s test accuracy

with respect to different leash tasks (i.e., HH, MH, and LH) on CIFAR-10 (non-IID Dir(0.1)). With the increase of τ from -1.5 to 3, the performance with the LH and MH leash tasks first increases and then decreases, while the performance with the HH leash task decreases monotonically. These results confirm the importance of choosing a low-heterogeneity task as the leash task and that the guiding strength should be too high or low to avoid “over leashing” or “under leashing”. This also suggests that one should decrease the guiding strength if the Leash-FL data heterogeneity is expected to be high. Note that even using randomly selected classes, the HH leash task can also improve over FedAvg with a carefully chosen τ around -1.

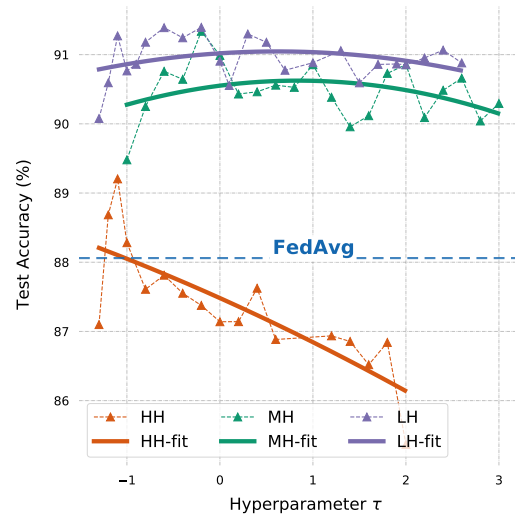


Figure 3. Test accuracy (%) of FedWalk under different τ with LH, MH, and MH leash tasks on CIFAR-10 (non-IID Dir(0.1)). The triangles represent the test accuracy while the cure lines highlight the approximated trends.

(2) Comparison with Pre-training. Here, we compare FedWalk with a pre-training approach that performs the leash training before FL starts. This experiment can help understand whether during-training leashing is better than pre-training leashing. Figure 4 illustrates the results where it shows that FedWalk (red bars) outperforms the pre-training (blue bars), especially under the non-IID setting. Particularly, under the non-IID (Dir(0.1)) setting, FedWalk surpasses pre-training by a margin of 2.05%, 2.23%, and 3.51% with HH, MH, and HH leash tasks, respectively. This verifies the necessity and importance of dual optimization of the leash and FL tasks for improved convergence.

(3) Impact of non-IID Level. Here, we conduct more experiments with FedWalk (with LH leash task) and FedAvg under different levels of FL data heterogeneity for $\alpha \in \{0.1, 0.3, 0.7, 1, 3, 10\}$. The results are shown in Figure 5. It can be observed that, while FedWalk demonstrates a consistent improvement over FedAvg, the superiority of

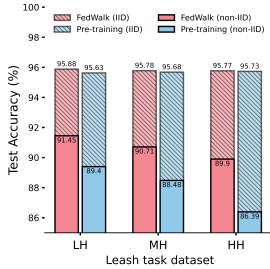


Figure 4. The test accuracy of FedWalk (red bars) and Pre-training (blue bars) on CIFAR-10 under both IID and non-IID settings.

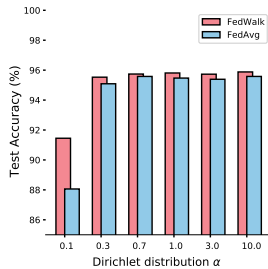


Figure 5. The test accuracy of FedWalk and FedAvg under different levels of FL data heterogeneity α on CIFAR-10 dataset.

FedWalk is more pronounced under higher levels of data heterogeneity, i.e., $\alpha = 0.1$. This highlights the importance of employing a server-side leash task to guide the FL task for high data heterogeneity FL tasks.

6. Conclusion

In this paper, we introduced a "Dog Walking Theory" to help analyze the convergence issues of FL and identify one key missing element in current FL algorithms, i.e., a leash task that can guide the convergence of the clients. We then proposed a novel FL method dubbed FedWalk that exploits an easy-to-converge task defined on a public dataset as the leash task to boost FL. We theoretically analyze the convergence benefit of FedWalk depending on the heterogeneity between the leash and FL tasks. The effectiveness of FedWalk was verified on CIFAR-10 and CIFAR-100 under both IID and non-IID settings. Our work reveals the importance of having a leash task in the current FL pipeline and opens up a new research direction for future research.

References

Acar, D. A. E., Zhao, Y., Navarro, R. M., Mattina, M., Whatmough, P. N., and Saligrama, V. Federated learning based on dynamic regularization. *arXiv preprint arXiv:2111.04263*, 2021.

Achiam, J., Adler, S., Agarwal, S., Ahmad, L., Akkaya, I., Aleman, F. L., Almeida, D., Altenschmidt, J., Altman, S., Anadkat, S., et al. Gpt-4 technical report. *arXiv preprint arXiv:2303.08774*, 2023.

Aggarwal, D., Zhou, J., and Jain, A. K. Fedface: Collaborative learning of face recognition model. 2021.

Ammad-Ud-Din, M., Ivannikova, E., Khan, S. A., Oyomno, W., Fu, Q., Tan, K. E., and Flanagan, A. Federated collaborative filtering for privacy-preserving personalized recommendation system. 2019.

Chai, Z., Ali, A., Zawad, S., Truex, S., Anwar, A., Baracaldo, N., Zhou, Y., Ludwig, H., Yan, F., and Cheng, Y. Tifi: A tier-based federated learning system. In *Proceedings of the 29th international symposium on high-performance parallel and distributed computing*, pp. 125–136, 2020.

Charles, Z. and Konečný, J. Convergence and accuracy trade-offs in federated learning and meta-learning. In *International Conference on Artificial Intelligence and Statistics*, pp. 2575–2583. PMLR, 2021.

Chen, H., Frikha, A., Krompass, D., Gu, J., and Tresp, V. Fraug: Tackling federated learning with non-iid features via representation augmentation. In *Proceedings of the IEEE/CVF International Conference on Computer Vision*, pp. 4849–4859, 2023.

Chen, H.-Y., Tu, C.-H., Li, Z., Shen, H. W., and Chao, W.-L. On the importance and applicability of pre-training for federated learning. In *The Eleventh International Conference on Learning Representations*, 2022.

Chen, X., Chen, T., Sun, H., Wu, S. Z., and Hong, M. Distributed training with heterogeneous data: Bridging median-and mean-based algorithms. *Advances in Neural Information Processing Systems*, 33:21616–21626, 2020.

Cho, Y. J., Gupta, S., Joshi, G., and Yağan, O. Bandit-based communication-efficient client selection strategies for federated learning. In *2020 54th Asilomar Conference on Signals, Systems, and Computers*, pp. 1066–1069. IEEE, 2020.

Crawshaw, M., Bao, Y., and Liu, M. Federated learning with client subsampling, data heterogeneity, and unbounded smoothness: A new algorithm and lower bounds. *Advances in Neural Information Processing Systems*, 36, 2024.

- Das, R., Acharya, A., Hashemi, A., Sanghavi, S., Dhillon, I. S., and Topcu, U. Faster non-convex federated learning via global and local momentum. In *Uncertainty in Artificial Intelligence*, pp. 496–506. PMLR, 2022.
- Devlin, J., Chang, M.-W., Lee, K., and Toutanova, K. Bert: Pre-training of deep bidirectional transformers for language understanding. *arXiv preprint arXiv:1810.04805*, 2018.
- Donevski, I., Nielsen, J. J., and Popovski, P. On addressing heterogeneity in federated learning for autonomous vehicles connected to a drone orchestrator. *Frontiers in Communications and Networks*, 2:709946, 2021.
- Fu, L., Zhang, H., Gao, G., Zhang, M., and Liu, X. Client selection in federated learning: Principles, challenges, and opportunities. *IEEE Internet of Things Journal*, 2023.
- He, C., Shah, A. D., Tang, Z., Sivashunmugam, D. F. N., Bhogaraju, K., Shimpi, M., Shen, L., Chu, X., Soltanolkotabi, M., and Avestimehr, S. Fedcv: a federated learning framework for diverse computer vision tasks. *arXiv preprint arXiv:2111.11066*, 2021.
- He, K., Zhang, X., Ren, S., and Sun, J. Deep residual learning for image recognition. In *Proceedings of the IEEE conference on computer vision and pattern recognition*, pp. 770–778, 2016.
- Hendrycks, D., Lee, K., and Mazeika, M. Using pre-training can improve model robustness and uncertainty. In *International conference on machine learning*, pp. 2712–2721. PMLR, 2019.
- Hsu, T.-M. H., Qi, H., and Brown, M. Measuring the effects of non-identical data distribution for federated visual classification. *arXiv preprint arXiv:1909.06335*, 2019.
- Jain, P., Kakade, S. M., Kidambi, R., Netrapalli, P., and Sidford, A. Accelerating stochastic gradient descent for least squares regression. In *Conference On Learning Theory*, pp. 545–604. PMLR, 2018.
- Kairouz, P., McMahan, H. B., Avent, B., Bellet, A., Bennis, M., Bhagoji, A. N., Bonawitz, K., Charles, Z., Cormode, G., Cummings, R., et al. Advances and open problems in federated learning. *Foundations and Trends® in Machine Learning*, 14(1–2):1–210, 2021.
- Karimireddy, S. P., Kale, S., Mohri, M., Reddi, S., Stich, S., and Suresh, A. T. Scaffold: Stochastic controlled averaging for federated learning. In *International conference on machine learning*, pp. 5132–5143. PMLR, 2020.
- Karimireddy, S. P., Jaggi, M., Kale, S., Mohri, M., Reddi, S., Stich, S. U., and Suresh, A. T. Breaking the centralized barrier for cross-device federated learning. *Advances in Neural Information Processing Systems*, 34:28663–28676, 2021.
- Khanduri, P., Sharma, P., Yang, H., Hong, M., Liu, J., Rajawat, K., and Varshney, P. Stem: A stochastic two-sided momentum algorithm achieving near-optimal sample and communication complexities for federated learning. *Advances in Neural Information Processing Systems*, 34:6050–6061, 2021.
- Kim, T., Bae, S., Lee, J.-w., and Yun, S. Accurate and fast federated learning via combinatorial multi-armed bandits. *arXiv preprint arXiv:2012.03270*, 2020.
- Krizhevsky, A., Hinton, G., et al. Learning multiple layers of features from tiny images. 2009.
- Lai, F., Zhu, X., Madhyastha, H. V., and Chowdhury, M. Oort: Efficient federated learning via guided participant selection. In *15th {USENIX} Symposium on Operating Systems Design and Implementation ({OSDI} 21)*, pp. 19–35, 2021.
- Li, C., Zeng, X., Zhang, M., and Cao, Z. Pyramidfl: A fine-grained client selection framework for efficient federated learning. In *Proceedings of the 28th Annual International Conference on Mobile Computing And Networking*, pp. 158–171, 2022a.
- Li, Q., He, B., and Song, D. Model-contrastive federated learning. In *Proceedings of the IEEE/CVF conference on computer vision and pattern recognition*, pp. 10713–10722, 2021.
- Li, Q., Diao, Y., Chen, Q., and He, B. Federated learning on non-iid data silos: An experimental study. In *2022 IEEE 38th International Conference on Data Engineering (ICDE)*, pp. 965–978. IEEE, 2022b.
- Li, T., Sahu, A. K., Zaheer, M., Sanjabi, M., Talwalkar, A., and Smith, V. Federated optimization in heterogeneous networks. *Proceedings of Machine learning and systems*, 2:429–450, 2020.
- Li, X., Huang, K., Yang, W., Wang, S., and Zhang, Z. On the convergence of fedavg on non-iid data. *arXiv preprint arXiv:1907.02189*, 2019.
- Malinovskiy, G., Kovalev, D., Gasanov, E., Condat, L., and Richtarik, P. From local sgd to local fixed-point methods for federated learning. In *International Conference on Machine Learning*, pp. 6692–6701. PMLR, 2020.
- McMahan, B., Moore, E., Ramage, D., Hampson, S., and y Arcas, B. A. Communication-efficient learning of deep networks from decentralized data. In *Artificial intelligence and statistics*, pp. 1273–1282. PMLR, 2017.

- McMahan, H. B., Moore, E., Ramage, D., and y Arcas, B. A. Federated learning of deep networks using model averaging, 2016. URL <https://arxiv.org/abs/1602.05629v1>.
- Nguyen, H. T., Sehwal, V., Hosseinalipour, S., Brinton, C. G., Chiang, M., and Poor, H. V. Fast-convergent federated learning. *IEEE Journal on Selected Areas in Communications*, 39(1):201–218, 2020.
- Nguyen, J., Malik, K., Sanjabi, M., and Rabbat, M. Where to begin? exploring the impact of pre-training and initialization in federated learning. *arXiv preprint arXiv:2206.15387*, 2022.
- Pathak, R. and Wainwright, M. J. Fedsplit: An algorithmic framework for fast federated optimization. *Advances in neural information processing systems*, 33:7057–7066, 2020.
- Reddi, S., Charles, Z., Zaheer, M., Garrett, Z., Rush, K., Konečný, J., Kumar, S., and McMahan, H. B. Adaptive federated optimization. *arXiv preprint arXiv:2003.00295*, 2020.
- Ribero, M. and Vikalo, H. Communication-efficient federated learning via optimal client sampling. *arXiv preprint arXiv:2007.15197*, 2020.
- Rombach, R., Blattmann, A., Lorenz, D., Esser, P., and Ommer, B. High-resolution image synthesis with latent diffusion models. In *Proceedings of the IEEE/CVF conference on computer vision and pattern recognition*, pp. 10684–10695, 2022.
- Rosenblatt, J. D. and Nadler, B. On the optimality of averaging in distributed statistical learning. *Information and Inference: A Journal of the IMA*, 5(4):379–404, 2016.
- Sheller, M. J., Edwards, B., Reina, G. A., Martin, J., and Bakas, S. Federated learning in medicine: facilitating multi-institutional collaborations without sharing patient data. *Scientific Reports*, 10(1), 2020.
- Tan, Y., Long, G., Ma, J., Liu, L., Zhou, T., and Jiang, J. Federated learning from pre-trained models: A contrastive learning approach. *Advances in Neural Information Processing Systems*, 35:19332–19344, 2022.
- Tan, Y., Liu, Y., Long, G., Jiang, J., Lu, Q., and Zhang, C. Federated learning on non-iid graphs via structural knowledge sharing. In *Proceedings of the AAAI conference on artificial intelligence*, volume 37, pp. 9953–9961, 2023.
- Wang, H., Yurochkin, M., Sun, Y., Papailiopoulos, D., and Khazaeni, Y. Federated learning with matched averaging. *arXiv preprint arXiv:2002.06440*, 2020a.
- Wang, J., Tantia, V., Ballas, N., and Rabbat, M. Slowmo: Improving communication-efficient distributed sgd with slow momentum. *arXiv preprint arXiv:1910.00643*, 2019.
- Wang, J., Liu, Q., Liang, H., Joshi, G., and Poor, H. V. Tackling the objective inconsistency problem in heterogeneous federated optimization. *Advances in neural information processing systems*, 33:7611–7623, 2020b.
- Wang, J., Xu, Z., Garrett, Z., Charles, Z., Liu, L., and Joshi, G. Local adaptivity in federated learning: Convergence and consistency. *arXiv preprint arXiv:2106.02305*, 2021.
- Wu, H. and Wang, P. Node selection toward faster convergence for federated learning on non-iid data. *IEEE Transactions on Network Science and Engineering*, 9(5): 3099–3111, 2022.
- Wu, X., Huang, F., Hu, Z., and Huang, H. Faster adaptive federated learning. In *Proceedings of the AAAI Conference on Artificial Intelligence*, volume 37, pp. 10379–10387, 2023.
- Xu, J., Wang, S., Wang, L., and Yao, A. C.-C. Fedcm: Federated learning with client-level momentum. *arXiv preprint arXiv:2106.10874*, 2021.
- Yuan, H., Zaheer, M., and Reddi, S. Federated composite optimization. In *International Conference on Machine Learning*, pp. 12253–12266. PMLR, 2021.
- Zhang, L., Shen, L., Ding, L., Tao, D., and Duan, L.-Y. Fine-tuning global model via data-free knowledge distillation for non-iid federated learning. In *Proceedings of the IEEE/CVF conference on computer vision and pattern recognition*, pp. 10174–10183, 2022.
- Zhao, Y., Li, M., Lai, L., Suda, N., Civin, D., and Chandra, V. Federated learning with non-iid data. *arXiv preprint arXiv:1806.00582*, 2018.
- Zhou, F. and Cong, G. On the convergence properties of a k -step averaging stochastic gradient descent algorithm for nonconvex optimization. *arXiv preprint arXiv:1708.01012*, 2017.
- Zinkevich, M., Weimer, M., Li, L., and Smola, A. Parallelized stochastic gradient descent. *Advances in neural information processing systems*, 23, 2010.

A. Appendix A: Proof of Theorem 4.9

A.1. Proof of Key Lemma

Lemma A.1. (Bounding the variance). Assume Assumption 4.3 holds. It follows that

$$\mathbb{E}[\|\bar{\mathbf{q}}_t - \mathbf{q}_t\|^2] \leq \sigma_s^2$$

Proof.

$$\mathbb{E}[\|\bar{\mathbf{q}}_t - \mathbf{q}_t\|^2] = \|\nabla F(\bar{\mathbf{W}}_t, \xi_t) - \nabla F(\bar{\mathbf{W}}_t)\|^2 \leq \sigma_s^2$$

□

A.2. Proof of Theorem 4.9

Proof. Notice that $\mathbf{W}_{t+1} = \mathbf{W}_t - \eta_t \mathbf{g}_t - \gamma_t \mathbf{q}_t$

$$\begin{aligned} & \|\mathbf{W}_{t+1} - \mathbf{W}^*\|^2 \\ &= \|\mathbf{W}_t - \eta_t \mathbf{g}_t - \gamma_t \mathbf{q}_t - \mathbf{W}^*\|^2 \\ &= \|\mathbf{W}_t - \eta_t \bar{\mathbf{g}}_t - \gamma_t \bar{\mathbf{q}}_t - \mathbf{W}^* + \eta_t \bar{\mathbf{g}}_t - \eta_t \mathbf{g}_t + \gamma_t \bar{\mathbf{q}}_t - \gamma_t \mathbf{q}_t\|^2 \\ &= \underbrace{\|\mathbf{W}_t - \eta_t \bar{\mathbf{g}}_t - \gamma_t \bar{\mathbf{q}}_t - \mathbf{W}^*\|^2}_{A1} \\ & \quad + \underbrace{\|\eta_t \bar{\mathbf{g}}_t - \eta_t \mathbf{g}_t + \gamma_t \bar{\mathbf{q}}_t - \gamma_t \mathbf{q}_t\|^2}_{A2} \\ & \quad + 2 \underbrace{\langle \mathbf{W}_t - \eta_t \bar{\mathbf{g}}_t - \gamma_t \bar{\mathbf{q}}_t - \mathbf{W}^*, \eta_t \bar{\mathbf{g}}_t - \eta_t \mathbf{g}_t + \gamma_t \bar{\mathbf{q}}_t - \gamma_t \mathbf{q}_t \rangle}_{A3} \end{aligned}$$

Note that $\mathbb{E}[A3] = 0$. We next focus on bounding A1 and A2.

$$\begin{aligned} A1 &= \|\mathbf{W}_t - \eta_t \bar{\mathbf{g}}_t - \gamma_t \bar{\mathbf{q}}_t - \mathbf{W}^*\|^2 \\ &= \|\mathbf{W}_t - \eta_t \bar{\mathbf{g}}_t - \mathbf{W}^*\|^2 + \gamma_t^2 \|\bar{\mathbf{q}}_t\|^2 \\ & \quad - 2\gamma_t \langle \mathbf{W}_t - \eta_t \bar{\mathbf{g}}_t - \mathbf{W}^*, \bar{\mathbf{q}}_t \rangle \end{aligned}$$

$$\begin{aligned} A2 &= \|\eta_t \bar{\mathbf{g}}_t - \eta_t \mathbf{g}_t + \gamma_t \bar{\mathbf{q}}_t - \gamma_t \mathbf{q}_t\|^2 \\ &= \eta_t^2 \|\bar{\mathbf{g}}_t - \mathbf{g}_t\|^2 + \gamma_t^2 \|\bar{\mathbf{q}}_t - \mathbf{q}_t\|^2 \\ & \quad + 2\gamma_t \eta_t \langle \bar{\mathbf{g}}_t - \mathbf{g}_t, \bar{\mathbf{q}}_t - \mathbf{q}_t \rangle \\ &= \eta_t^2 \|\bar{\mathbf{g}}_t - \mathbf{g}_t\|^2 + \gamma_t^2 \|\bar{\mathbf{q}}_t - \mathbf{q}_t\|^2 \end{aligned}$$

Then

$$\begin{aligned} & \|\mathbf{W}_{t+1} - \mathbf{W}^*\|^2 \\ &= \|\mathbf{W}_t - \eta_t \bar{\mathbf{g}}_t - \mathbf{W}^*\|^2 - 2\gamma_t \langle \mathbf{W}_t - \eta_t \bar{\mathbf{g}}_t - \mathbf{W}^*, \bar{\mathbf{q}}_t \rangle \\ & \quad + \eta_t^2 \|\bar{\mathbf{g}}_t - \mathbf{g}_t\|^2 + \gamma_t^2 \|\bar{\mathbf{q}}_t - \mathbf{q}_t\|^2 + \gamma_t^2 \|\bar{\mathbf{q}}_t\|^2 \\ &= \|\mathbf{W}_t - \eta_t \bar{\mathbf{g}}_t - \mathbf{W}^*\|^2 + \eta_t^2 \|\bar{\mathbf{g}}_t - \mathbf{g}_t\|^2 + \gamma_t^2 \|\bar{\mathbf{q}}_t\|^2 \\ & \quad - 2\eta_t \langle \mathbf{W}_t - \eta_t \bar{\mathbf{g}}_t - \mathbf{W}^*, \bar{\mathbf{g}}_t - \mathbf{g}_t \rangle \\ & \quad - 2\gamma_t \langle \mathbf{W}_t - \eta_t \bar{\mathbf{g}}_t - \mathbf{W}^*, \bar{\mathbf{q}}_t \rangle \\ & \quad + 2\eta_t \langle \mathbf{W}_t - \eta_t \bar{\mathbf{g}}_t - \mathbf{W}^*, \bar{\mathbf{g}}_t - \mathbf{g}_t \rangle + \gamma_t^2 \|\bar{\mathbf{q}}_t - \mathbf{q}_t\|^2 \\ &= \|\mathbf{W}_t - \eta_t \bar{\mathbf{g}}_t - \mathbf{W}^* + \eta_t \bar{\mathbf{g}}_t - \eta_t \mathbf{g}_t\|^2 \\ & \quad - 2\gamma_t \langle \mathbf{W}_t - \eta_t \bar{\mathbf{g}}_t - \mathbf{W}^*, \bar{\mathbf{q}}_t \rangle \\ & \quad - 2\eta_t \langle \mathbf{W}_t - \eta_t \bar{\mathbf{g}}_t - \mathbf{W}^*, \bar{\mathbf{g}}_t - \mathbf{g}_t \rangle \\ & \quad + \gamma_t^2 \|\bar{\mathbf{q}}_t\|^2 + \gamma_t^2 \|\bar{\mathbf{q}}_t - \mathbf{q}_t\|^2 \\ &= \|\mathbf{W}_t - \eta_t \bar{\mathbf{g}}_t - \mathbf{W}^* + \eta_t \bar{\mathbf{g}}_t - \eta_t \mathbf{g}_t\|^2 \\ & \quad - 2\gamma_t \langle \mathbf{W}_t - \eta_t \bar{\mathbf{g}}_t - \mathbf{W}^*, \bar{\mathbf{q}}_t \rangle \\ & \quad + \gamma_t^2 \|\bar{\mathbf{q}}_t\|^2 + \gamma_t^2 \|\bar{\mathbf{q}}_t - \mathbf{q}_t\|^2 \\ &= \underbrace{\|\mathbf{W}_t - \mathbf{W}^* - \eta_t \mathbf{g}_t\|^2}_{FedAvg} - 2\gamma_t \underbrace{\langle \mathbf{W}_t - \eta_t \bar{\mathbf{g}}_t - \mathbf{W}^*, \bar{\mathbf{q}}_t \rangle}_{B1} \\ & \quad + \gamma_t^2 \|\bar{\mathbf{q}}_t\|^2 + \gamma_t^2 \|\bar{\mathbf{q}}_t - \mathbf{q}_t\|^2 \end{aligned}$$

where $\mathbb{E}(\langle \mathbf{W}_t - \eta_t \bar{\mathbf{g}}_t - \mathbf{W}^*, \bar{\mathbf{g}}_t - \mathbf{g}_t \rangle) = 0$.

Next, we focus on bounding B1,

$$\begin{aligned} B1 &= -2\gamma_t \langle \mathbf{W}_t - \eta_t \bar{\mathbf{g}}_t - \mathbf{W}^*, \bar{\mathbf{q}}_t \rangle \\ &= -2\gamma_t \langle \bar{\mathbf{W}}_t - \mathbf{W}^*, \bar{\mathbf{q}}_t \rangle \\ &= \underbrace{-2\gamma_t \langle \bar{\mathbf{W}}_t - \mathbf{W}_s^*, \nabla F(\bar{\mathbf{W}}_t) \rangle}_{C1} \\ & \quad - \underbrace{2\gamma_t \langle \mathbf{W}_s^* - \mathbf{W}^*, \nabla F(\bar{\mathbf{W}}_t) \rangle}_{C2} \end{aligned}$$

$$\begin{aligned} C1 &= -2\gamma_t \langle \bar{\mathbf{W}}_t - \mathbf{W}_s^*, \nabla F(\bar{\mathbf{W}}_t) \rangle \\ &\leq 2\gamma_t (F^* - F(\bar{\mathbf{W}}_t)) - \frac{\gamma_t}{L} \|\bar{\mathbf{q}}_t\|^2 \end{aligned}$$

$$\begin{aligned} C2 &= -2\gamma_t \langle \mathbf{W}_s^* - \mathbf{W}^*, \nabla F(\bar{\mathbf{W}}_t) \rangle \\ &\leq \|\mathbf{W}_s^* - \mathbf{W}^*\|^2 + \gamma_t^2 \|\bar{\mathbf{q}}_t\|^2 \\ &\leq \frac{2}{\mu} (F(\mathbf{W}^*) - F(\mathbf{W}_s^*)) + \gamma_t^2 \|\bar{\mathbf{q}}_t\|^2 \\ &= \frac{2}{\mu} (f^* - F^*) + \gamma_t^2 \|\bar{\mathbf{q}}_t\|^2 \\ &= \frac{2}{\mu} \Gamma_s + \gamma_t^2 \|\bar{\mathbf{q}}_t\|^2, \end{aligned}$$

where the first inequality is a result from *AM-GM* inequality, the second inequality is from μ -strong assumption, and we use the notation $\Gamma_s = f^* - F^*$.

Then, we have

$$B1 \leq (\gamma_t^2 - \frac{\gamma_t}{L}) \|\bar{\mathbf{q}}_t\|^2 + \frac{2}{\mu} \Gamma_s + 2\gamma_t (F^* - F(\bar{\mathbf{W}}_t))$$

So,

$$\begin{aligned} & \mathbb{E} \|\mathbf{W}_{t+1} - \mathbf{W}^*\|^2 \\ &= \underbrace{\mathbb{E} \|\mathbf{W}_t - \mathbf{W}^* - \eta_t \mathbf{g}_t\|^2}_{FedAvg} \\ & \quad + \underbrace{\frac{2}{\mu} \Gamma_s + \gamma_t^2 \mathbb{E} \|\bar{\mathbf{q}}_t - \mathbf{q}_t\|^2 - 2\gamma_t (F(\bar{\mathbf{W}}_t) - F^*)}_{D1} \\ & \quad - \underbrace{(\frac{\gamma_t}{L} - 2\gamma_t^2) \mathbb{E} \|\bar{\mathbf{q}}_t\|^2}_{D2} \end{aligned}$$

$$\begin{aligned} & D1 + D2 \\ &= \gamma_t^2 \mathbb{E} [\|\bar{\mathbf{q}}_t - \mathbf{q}_t\|^2] + \frac{2}{\mu} \Gamma_s - 2\gamma_t (F(\bar{\mathbf{W}}_t) - F^*) \\ & \quad - (\frac{\gamma_t}{L} - 2\gamma_t^2) \mathbb{E} [\|\bar{\mathbf{q}}_t\|^2] \\ &= \gamma_t^2 \sigma_s^2 - (4\gamma_t - 4L\gamma_t^2) (F(\bar{\mathbf{W}}_t) - F^*) + \frac{2}{\mu} \Gamma_s \\ &= \gamma_t^2 \sigma_s^2 + \frac{2}{\mu} \Gamma_s - (4\gamma_t - 4L\gamma_t^2) (F(\bar{\mathbf{W}}_t) - f^* + f^* - F^*) \\ &= \gamma_t^2 \sigma_s^2 + (\frac{2}{\mu} + 4L\gamma_t^2 - 4\gamma_t) \Gamma_s \\ & \quad - (4\gamma_t - 4L\gamma_t^2) (F(\bar{\mathbf{W}}_t) - f^*) \end{aligned}$$

The result is

$$\begin{aligned} & \mathbb{E} \|\mathbf{W}_{t+1} - \mathbf{W}^*\|^2 \\ &= \underbrace{\mathbb{E} \|\mathbf{W}_t - \mathbf{W}^* - \eta_t \mathbf{g}_t\|^2}_{FedAvg} \\ & \quad + \gamma_t^2 \sigma_s^2 + (\frac{2}{\mu} + 4L\gamma_t^2 - 4\gamma_t) \Gamma_s - (4\gamma_t - 4L\gamma_t^2) \Pi, \end{aligned}$$

where $\Pi = F(\bar{\mathbf{W}}_t) - f^*$.

□

B. Appendix B: Experimental details

Following a typical setup of FL, we assume the meta information of the FL task is known to the server, e.g., the class names of the classification task. When the class names are unavailable, the server can request the clients to upload their associated concepts to the server. The server uses this meta

information to find the most similar concepts in a public dataset (e.g., ImageNet-1k) with the assistance of GPT-4. When no closely related public datasets are available, the server can leverage a diffusion model to generate images with similar concepts. In this work, we only focus on the case that a large-scale public dataset is at hand to create the leash task. Next, we describe the selection process of the CIFAR-10 and CIFAR-100 leash tasks in detail.

B.1. CIFAR-10 Leash Task

Here, we present the prompt and GPT-4 answer used to find the most similar classes in the ImageNet-1K dataset ForCIFAR-10 FL task.

Prompt: "For each concept in the following "Client Label List", please select the top four most relevant labels from the above "Reference Label List". Please sort the selected labels for each concept and return them as a dictionary with the concept as the key and the top 4 most relevant labels as a list of values. You should return 40 labels in total. Client Label List: {1: 'airplane', 2: 'automobile', 3: 'bird', 4: 'cat', 5: 'deer', 6: 'dog', 7: 'frog', 8: 'horse', 9: 'ship', 10: 'truck'}."

GPT-4 Answer: {'airplane': lable1, label2, label3, label4. }, ..., {'truck': lable1, label2, label3, label4. }

The selected ImageNet classes are listed in Table 3. We then select the top 2 classes to construct the LH leash task. For the MH leash task, we replace the top 10-20 classes with 10 randomly selected ImageNet classes. For the HH leash task, we randomly select 20 classes from ImageNet. The specific classes of the leash tasks are listed in **The Result** below Table 3.

Table 3. The top 4 most relevant labels of ImageNet-1K for each CIFAR-10 class found by GPT-4.

CIFAR-10	ImageNet-1k
airplane	{"n04552348", "n02690373", "n02687172", "n04552348" }
automobile	{"n02814533", "n03100240", "n03594945", "n04467665" }
bird	{"n01796340", "n01797886", "n01608432", "n01795545" }
cat	{"n02124075", "n02123597", "n02123045", "n02123394" }
deer	{"n02437616", "n02412080", "n02415577", "n02396427" }
dog	{"n02085782", "n02085620", "n02085620", "n02085936" }
frog	{"n01644900", "n01644373", "n01641577", "n01910747" }
horse	{"n02389026", "n02391049", "n02412080", "n02504458" }
ship	{"n03673027", "n02981792", "n03095699", "n03673027" }
truck	{"n03417042", "n04467665", "n03777568", "n03770679" }

The Result. The labels (class indexes of ImageNet-1k) of the leash tasks found for the CIFAR-10 dataset:

- **LH:**

["n01644900", "n04552348", "n03673027",
"n02814533", "n03417042", "n02124075",
"n02389026", "n01796340", "n02085782",

```
"n02437616", "n01644373", "n02690373",
"n02981792", "n03100240", "n04467665",
"n02123597", "n02391049", "n01797886",
"n02085620", "n02412080"]
```

• **MH:**

```
["n01644900", "n04552348", "n03673027",
"n02814533", "n03417042", "n02124075",
"n02389026", "n01796340", "n02085782",
"n02437616", "n01440764", "n01692333",
"n02279972", "n02480495", "n01753488",
"n04356056", "n03637318", "n02132136",
"n01697457", "n04501370"]
```

• **HH :**

```
["n01518878", "n01692333", "n01776313",
"n02033041", "n02086079", "n02124075",
"n02236044", "n02279972", "n02480495",
"n02497673", "n03188531", "n03443371",
"n03637318", "n03786901", "n04111531",
"n04285008", "n04318186", "n04356056",
"n04501370", "n0685654"]
```

B.2. CIFAR-100 Leash Task

For CIFAR-100, we only construct an LH leash task of 40 classes following the same procedure as above. The labels (class indexes of ImageNet-1k) of the leash task are:

```
['n01484850', 'n01729322', 'n01667778', 'n11939491',
'n03063599', 'n02708093', 'n03388549', 'n02276258',
'n02132136', 'n02504013', 'n04311004', 'n02437312',
'n02119022', 'n01978287', 'n02804414', 'n02342885',
'n03478589', 'n02066245', 'n07742313', 'n09193705',
'n03792782', 'n02077923', 'n07730033', 'n03775546',
'n07734744', 'n03187595', 'n04344873', 'n02165456',
'n02129604', 'n02980441', 'n02894605', 'n02403003',
'n02509815', 'n01944390', 'n03763968', 'n03272562',
'n04465501', 'n12057211', 'n11879895', 'n03785016'].
```